LA-UR-99-1363

Effect of the Plutonium α–β Phase Transition Expansion on Storage Can Integrity: Experimental Results

Dane R. Spearing, NMT-6
D. Kirk Veirs, NMT-6

March 25, 1999

Los Alamos
National Laboratory

Los Alamos National Laboratory is operated by the University of California for the United States Department of Energy under contract W-7405-ENG-36.

This work was supported by the Nuclear Materials Stewardship Project Office of the US Department of Energy.

An Affirmative Action/Equal Opportunity Employer

Effect of the Plutonium $\alpha-\beta$ Phase Transition Expansion on Storage Can Integrity: Experimental Results

LA-UR-99-1363

Dane R. Spearing and D. Kirk Veirs

Nuclear Materials Technology Division
Los Alamos National Laboratory
Los Alamos, NM 87545

ABSTRACT

This study was performed to experimentally determine the effects of the volume expansion of plutonium metal undergoing the alpha to beta phase transition on a stainless steel storage container of the type specified by the Department of Energy plutonium storage standard (DOE, 1996). A monolithinc cylindrical plutonium ingot was placed in the axial center of an annealed stainless steel cylinder with an inner diameter 0.004” larger than the outer diameter of the ingot. The geometry maximizes the strength of the plutonium ingot with respect to the confining stainless steel cylinder and represents a “worst case” geometry for assessing the possibility of containment failure. The ingot was thermally cycled until equilibrium in the strain response was reached at six cycles. Based the experimental results detailed herein, the total strain that was imparted to the stainless steel cylinder through six thermal cycles was 2.03% and expansion of the ingot in the axial direction was measured to be greater than 5%, as compared to 3% for each direction expected for isotropic expansion. Elastic strain was measured to be ~0.2%.

INTRODUCTION

The current US Department of Energy (DOE) standard for the stabilization, packaging, and storage of plutonium bearing materials (DOE, 1996) specifies a maximum temperature of 100°C for the storage of alpha-phase Pu metal (α-Pu). The rationale for this maximum temperature was to address the possibility of compromising the integrity of the standard-specified stainless steel storage cans due to the large volume expansion (~10%) associated with the plutonium alpha to beta phase transition, which occurs at ~120°C. The assumption was that pieces of α-Pu metal tightly fit within the container had the potential for deforming the wall of a storage container beyond accepted criteria (ASME, 1995) upon transforming to β-Pu and/or via repeated cycling through the α/β transition. Within current proposed storage facilities (such as the Actinide Storage Facility at the Savannah River Site), credible scenarios exist in which local temperatures could significantly exceed the Pu α/β transition temperature. (As an example, the cooling system could fail and self-heating and insulating conditions could raise the plutonium metal temperature above 120°C). Thus, the purpose of this study was to experimentally determine the effects of the volume expansion of the alpha to beta transformation of plutonium metal on a stainless steel storage container of the type specified by the plutonium storage standard. This report gives a detailed description of the experimental set-up and run conditions as well as plots of all of the raw temperature and strain gage data. A review of the relevant literature and analysis of the data was reported by Spearing et al.(1999). Further analysis of the data using finite element analysis (FEA) modeling was reported by Flanders (1999).

EXPERIMENTAL PROCEDURE

The Pu source material used for this experiment was supplied by Savannah River, and consists of high-purity alpha phase metal with an average total impurity content of 432 ppm (exclusive of Am), and an average isotopic concentration of 93.83% ^{239}Pu. Based on the starting ^{241}Pu concentration and the age of the material, the total Americium concentration was calculated to be about 1500 ppm. The material was melted and chill cast at the plutonium foundry at Los Alamos

National Laboratory into a graphite mold, which resulted in an as-cast cylindrical ingot 4.51” in diameter and 0.78” in height, with a mass of 4231.3 g. Following casting, the ingot was machined to a right circular cylinder of the following dimensions: 4.358” diameter, 0.751” thickness, 3591.7 g mass (Figure 1). Using an immersion method, the density was measured to be 19.57 g/cc. The high measured density (theoretical max. $\rho_{\alpha-Pu}$= 19.86 g/cc) and surface uniformity of the cast ingot indicated the absence of any significant microcracking or void space formation from the casting process. Previous studies indicate that the presence of certain impurities, such as Am, on the order of 1000 ppm, drastically reduce microcrack formation during casting (Nelson, 1966). Thus, the 1500 ppm Am content of the material used in this study may in part be responsible for the observed high density and lack of significant microcracking.

In order to simplify subsequent finite element analyses of the experimental results (Flanders, 1999) and eliminate any contribution to the wall strength of the container by a bottom or lid, a steel cylinder was used to simulate a DOE standard 3013 inner canister. Several of these cylinders were manufactured at the Savannah River Site (SRS) using 316 stainless steel via a process which resulted in a fully annealed product (no remnant work hardening of the steel). The cylinders were then machined to right circular cylinders. The cylinder used for this experiment was designated as SRS Part #3, and had dimensions reported by SRS as the following: 4.359” internal diameter (ID), 4.486” outer diameter (OD), 6.008” length, 0.060” thickness. The ID was re-measured upon arrival at LANL as 4.362”, which leaves a 0.002” radial clearance between the Pu ingot and ID of the cylinder.

Twelve strain gages, the locations of which are shown in Figure 2, were installed on the outer surface of the cylinder as per the manufacturer’s (Micro-Measurements Division, Measurements Group, Inc., Raleigh, NC) instructions. (All strain gage related parts listed below are from this manufacturer.) Note that through the course of the experiment, several different numbering schemes were used in labeling the strain gages. Table 1 shows the correlation between the strain gage numbers using in this report with those used in the report by Flanders (1999). The cylinder exterior was first cleaned with ethanol to remove oils or other organics followed by dry abrading

with 320 grit emory cloth. The surface was then cleaned with M-Prep Conditioner A (a phosporic acid based cleaning agent) while abrading with 320 grit emory cloth. The abraded material was removed with cotton swabs soaked in M-Prep Conditioner A. A wipe was then used to remove any liquid resulting in a dry surface. The acid on the surface was neutralized using M-Prep Neutralizer 5A (an ammonia based neutralizer).

Three types of strain gages were used. Small single direction gages (part EP-08-062-DN-350) were chosen to measure the equatorial strain at the position on the tube corresponding to the axial middle of the puck. Two inch long single direction gages (part EA-06-20CRW-120) were chosen to measure the axial strain across the entire height of the puck. A two-element 90 degree rosette was chosen to measure the axial and equatorial strains in a region on the tube far from the puck.

The first eight gages were aligned to obtain equatorial strain along the center line of the puck, gages 9 and 10 were aligned to obtain axial strain across the puck, and gages 11 and 12 were aligned to obtain axial and equatorial strain away from the puck (height of center of gage at 115 mm). The gages were bonded to the stainless steel using M-Bond 600, an epoxy good to 370 °C. The epoxy was cured at 75 °C for at least 12 hours. A Type C solder pad was used with each gage, the pads being connected to the gage via a single strain-relieved wire. The solder pads were then connected to the instrumentation using a three conductor, 30 gauge twisted cable with etched Teflon insulation rated to 260 °C (330-FTE). The solder used was a 63% tin/36.65% lead/0.35% antimony solder, which is good to 183 °C (361A-20R). The three wire configuration was used to prevent thermal drift due to resistance changes in the leads as the temperature changes. The open faced gages (EP-08-062-DN-350 and EA-06-20CRW-120) were coated with the adhesive to protect the gage during installation. After installation, all gages were coated with a silicon rubber environmental coating (M-Coat C), rated to 290 °C. The continuity of the wiring was checked after installation, and it was found that gages 2 and 4 could not be used due to bad installation; gage 2 had an open circuit and gage 4 was visibly damaged during installation.

Three K-type thermocouples (Model SA1-K, Omega, Inc.) were placed on the outside of the can in positions illustrated in Figure 2. A fourth thermocouple was placed on the Pu ingot itself

during the experiment. The thermocouples were attached via self-adhesive pads which are certified for use up to 160°C. Prior to use, the thermocouples were calibrated in a controlled environment between 0° - 160°C using equipment traceable to national standards by the LANL Standards and Calibration Laboratory, and certified to be accurate to ±0.3°C. Output leads from the strain gages and thermocouples were connected to a National Instruments SCXI-1321Terminal Block. Strain and temperature data recorded at 15 second intervals during the experiment via a custom written LabView software application.

The furnace used was a Lindberg MK-6015-S, 208V 4000W horizontal open-ended tube furnace, 15" long, 6" ID with a custom built temperature controller. For all thermal cycles, heating was done from ambient temperature to 130°C at 2°C/min. Cooling was done by turning off the furnace power and letting the experiment cool to ambient. All experiments took place within an Ar-atmosphere glovebox, with O_2 levels maintained at 30 ppm or less.

Following installation of the furnace and steel cylinder into the glovebox, several strips of fiberglass cloth were laid down inside the bottom half of the tube furnace on which the cylinder was placed. This prevented direct contact of the outside of the cylinder, as well as the strain gages and thermocouples, with the heating elements of the furnace.

Thickness changes in the Pu ingot were measured using two quartz glass rod dilatometers attached to dial indicators (Part #196B, Starrett Co.), accurate to ±0.001". Readings from the dial indicators were recorded manually throughout the course of the experiments. One of the dilatometers is shown in Figure 3 and a schematic of the entire experimental setup is given in Figure 4.

Prior to performing the experiment using the Pu ingot, a "dry run" was done in order to quantify the thermal response behavior of the strain gages. A brass ingot, of the same dimensions as the Pu ingot, was slid into the steel cylinder and centered by hand to act as a thermal mass. The cylinder and brass ingot were then thermally cycled in a manner identical to which the Pu ingot would be cycled (2°C/min heating rate to 150°C, 30-90 minutes at 150°C, followed by power-off cooling to ambient temperature) and the response of the strain gages recorded as a function of time

and temperature. Note that no additional strains were applied to the cylinder by the brass ingot, which was used solely as a thermal mass. Results are plotted in Figure 5. The far-field and axial strain gages (9,10,11,12) showed a positive strain in response to temperature of 550±20 microstrain (με) from ambient to 130°C. The hoop strain gages showed negative strain in response to temperature of –250±20με from ambient to 130°C except for strain gage #1 which showed –170±20με.

Following the dry run, the brass ingot was removed from the cylinder and the Pu ingot was inserted by hand (see Figure 6), a thermocouple was attached to the ingot, and the ingot was centered within cylinder with the aid of a ruler to within ±1 mm. The cylinder was oriented in the furnace with thermocouple T1 at the bottom, and thermocouple T3 and the far-field strain gages (11,12) at the top. Quartz glass rod dilatometers were then placed on the opposing faces of the ingot and zeroed. All strain gages were zeroed prior to the first thermal cycle. This is the only time the strain gages were zeroed so that the cumulative effects of strain as a function of cycle could be measured.

RESULTS

NOTE: The raw data files from these experiments are available on the web at:
http://www.lanl.gov/projects/pumatsci/

The strain and temperature vs. time data for all cycles are given in Figures 7 – 12. All of the hoop strain gages (1,3,5,6,7,8) showed peak positive strains for all cycles. In contrast, the longitudinal gages (9,10) showed slight negative strains. The far-field gages (11,12) showed only the expected thermal response of the empty cylinder, indicating no additional strain was accumulated away from the area in which the ingot was in contact with the cylinder. The temperature data presented in Figures 7 – 12 is from the thermocouple placed on the plutonium ingot. Based on this first cycle, the calculated total strain on the steel cylinder averaged among all

hoop strain gages is 1.44%. As is evident from Figure 7, a large proportion of this strain is plastic (1.27% average), given that only a small amount of strain relaxation is observed after cooling. Subtracting the plastic from the total strain leaves the elastic strain, which is 0.17% on average for the first cycle.

Between the end of first the first cycle and the beginning of the second cycle, strain gage #7 exhibited an anomalous 8430 με decrease in observed strain. The reason for this decrease is unclear at this point (e.g. – a delamination of the strain gage would result in no strain response in subsequent experiments, yet a positive strain response is still observed). Thus, we recommend that the data from this strain gage not be used in calculating average strain values for any cycle after the first.

A plot of the temperature recorded by the three thermocouples on the outside of the cylinder as a function of the thermocouple on the Pu ingot inside the cylinder between ambient and 115°C upon heating (i.e. - prior to temperature effects induced by the phase transition) for the first cycle is given in Figure 13. Thermocouple 1, which was placed on the bottom of the cylinder, consistently shows a higher temperature relative to the ingot than the thermocouples placed on the side and top of the cylinder. This is no doubt due to its closer proximity to the furnace heating elements relative to the other thermocouples, which is confirmed by the furnace controller induced oscillations in the observed temperature for this thermocouple. During the course of the first cycle, the temperature output from thermocouple #1 also exceeded the maximum temperature setting of the data collection program (154.5°C). Although the maximum temperature for this region of the cylinder was thus not recorded, it is estimated to be < 170°C based on the trend of the data from the other thermocouples. Following the first cycle, this thermocouple was disconnected and one of the furnace control thermocouples was recorded in its place.

A plot of strain vs. time for all six cycles for strain gage #3, which consistently showed the highest strain levels, is given in Figure 14. Six regimes of the strain vs. time plot for the first cycle are identified and interpreted as follows: (1) the first regime labeled represents strain accumulated due to the thermal expansion of α-Pu. Prior to this point, the flat part of the curve represents the

time before the furnace was turned on, and the small amount of expansion of the α-Pu needed to close the 0.002” radial gap between the ingot and inside of the cylinder. The strain rate between 80°C – 110°C, averaged among all hoop gages, is 34.7 ± 4.7 με/°C, which is in reasonable agreement with the published linear thermal expansion value for alpha-Pu of 42.3 με/°C (Miner and Schonfeld, 1980). (2) At about 120 minutes into the run, the slope of the strain vs. time curve increases, and the second region represents strain accumulation due to expansion associated with the α to β phase transition. Essentially all of the thermal energy is consumed by the endothermic α to β phase transition, and thus the temperature does not increase significantly during this time, as can be seen in Figure 8. This is characteristic behavior of first order phase transitions. (3) The strain peaks at the end of the phase transition, and then decreases slightly as the temperature is held constant. This strain decrease is most likely due to creep of the β-phase under the pressures imposed by the walls of the cylinder. (4) Once the furnace is turned off, a slight decrease in strain is observed due to thermal contraction of the β-phase. In this region, the strain rate is 16.7 ± 0.4 με/°C, which is in good agreement with the thermal contraction of β-Pu along the b-axis: 14 με/°C (Miner and Schonfeld, 1980). (5) This is followed by a small but sharp drop in strain due to the β to α phase transition. Note that during the β to α phase transition, the temperature of the Pu ingot also increases slightly due to the release of the latent heat of the exothermic β to α phase transition (see Figure 8). (6) Following the β–α phase transition, no further change in the strain is measured indicating that the cylinder was plastically deformed during this cycle.

As is evident from Figure 14, most plastic strain in the cylinder is accumulated during the first thermal cycle. With each subsequent cycle, the amount of additional accumulated plastic strain decreases until cycle 6, in which no additional plastic strain is observed. Plots of the total, plastic, and elastic strain accumulated within each cycle based on strain gage #3 are given in Figure 15 (representing the highest observed “worst case” strain data). The total amount of plastic strain observed for all cycles, obtained by summing the amount of plastic strain accumulated during each cycle for strain gage #3, is 2.03%.

Dilatometry data is presented for the first and fourth cycle in Figures 16 and 17, respectively. The change in thickness of the ingot was calculated by adding the measurements from the two opposing dilatometers. In Figure 16, both the change in thickness of the ingot and the strain from gage #3 are plotted as a function of temperature. A small increase in thickness (0.001", 0.13%) was observed prior to the onset of the phase transition, which is consistent within error with the linear thermal expansion expected for α-Pu (~0.5%) over the temperature range from ambient to 110°C (Miner and Schonfeld, 1980). Starting at the onset of the phase transition, as indicated by the sharp increase in strain, the thickness increased by 0.042" (5.8%) during heating. This is nearly twice the expected linear thermal expansion (~3%) for the volume expansion associated with the α to β phase transition.

In Figure 17, the strain from gage #3 and the thickness change are plotted as a function of time for the fourth cycle. Prior to the onset of the phase transition, a marked *decrease* in thickness (–1.8%) was observed, followed by a modest thickening of the ingot of 0.6% (over the starting thickness) during and after the phase transition.

Following the sixth thermal cycle, the ingot was removed from the cylinder and the cylinder outer diameter at the midpoint was measured to have increased by 0.071". Based on an initial OD of 4.477", this represents a 1.58% increase in circumference, in good agreement with the measured strain of 1.32% averaged over all hoop gages. The plastic deformation is visible as a slight bulge in the center of the cylinder, as evident in Figure 18. Despite the low oxygen levels generally maintained in the glovebox (< 30ppm), the Pu ingot showed surface oxidation upon removal from the cylinder (Figure 19). This oxidation may have been a result of above ambient temperatures, and thus higher reactivity, or due to a single overnight loss of negativity in the glovebox which resulted in significantly higher O_2 levels. Despite the coating of oxide, the ingot was still intact as a single massive piece of metal following the experiment with no obvious signs of severe cracking.

DISCUSSION & CONCLUSIONS

Further analysis of the data and resulting conclusions was reported previously by Spearing et al. (1999), and Finite Element Analysis modeling of the experiment was reported by Flanders (1999).

ACKNOWLEDGEMENTS

The authors would like to thank Arthur "Lonny" Morgan and Ann Schake for their invaluable assistance in setting up and conducting this study. We are also greatly indebted to the following LANL Plutonium Foundry personnel for their outstanding efforts in casting and machining the plutonium ingot used in this experiment: John Huang, Charles Puglisi, Kenny Vigil, Anthony Valdez, Floyd Rodriguez, Theresa Abeyta, Steve Boggs, and Pat Rodriguez. This work was supported by the Nuclear Materials Stewardship Project Office of the United States Department of Energy.

REFERENCES CITED

ASME (1995) Section VIII, Division 2. In Boiler and Pressure Vessle Code, p. American Society of Mechanical Engineers.

DOE (1996). Criteria for preparing and packaging plutonium metals and oxides for long-term storage No. DOE-STD-3013-96. Department of Energy.

Flanders, H.E. (1999). Plutonium alpha-beta expansion & BNFL (3013) inner and outer storage cans evaluation. Report No. T-CLC-G-00113. Westinghouse Savannah River Company.

Miner, W.N., and Schonfeld, F.W. (1980) Physical Properties. In O. J. Wick (eds), Plutonium Handbook, p. 31-57. American Nuclear Society, La Grange Park, IL.

Nelson, R.D. (1966) Phase transformation damage in plutonium. Journal of Nuclear Materials, 20, 153-161.

Spearing, D.R., Veirs, D.K., and Prenger, F.C. (1999). Effect of the plutonium α–β phase transition expansion on storage can integrity. Report No. LA-UR-99-147. Los Alamos National Laboratory.

This Report	Flanders (1999)
1	1
3	2
5	8
6	7
7	6
8	5
9	9
10	10
11	3
12	4

Table 1 – Correlation between strain gages numbers from this report and Flanders (1999).

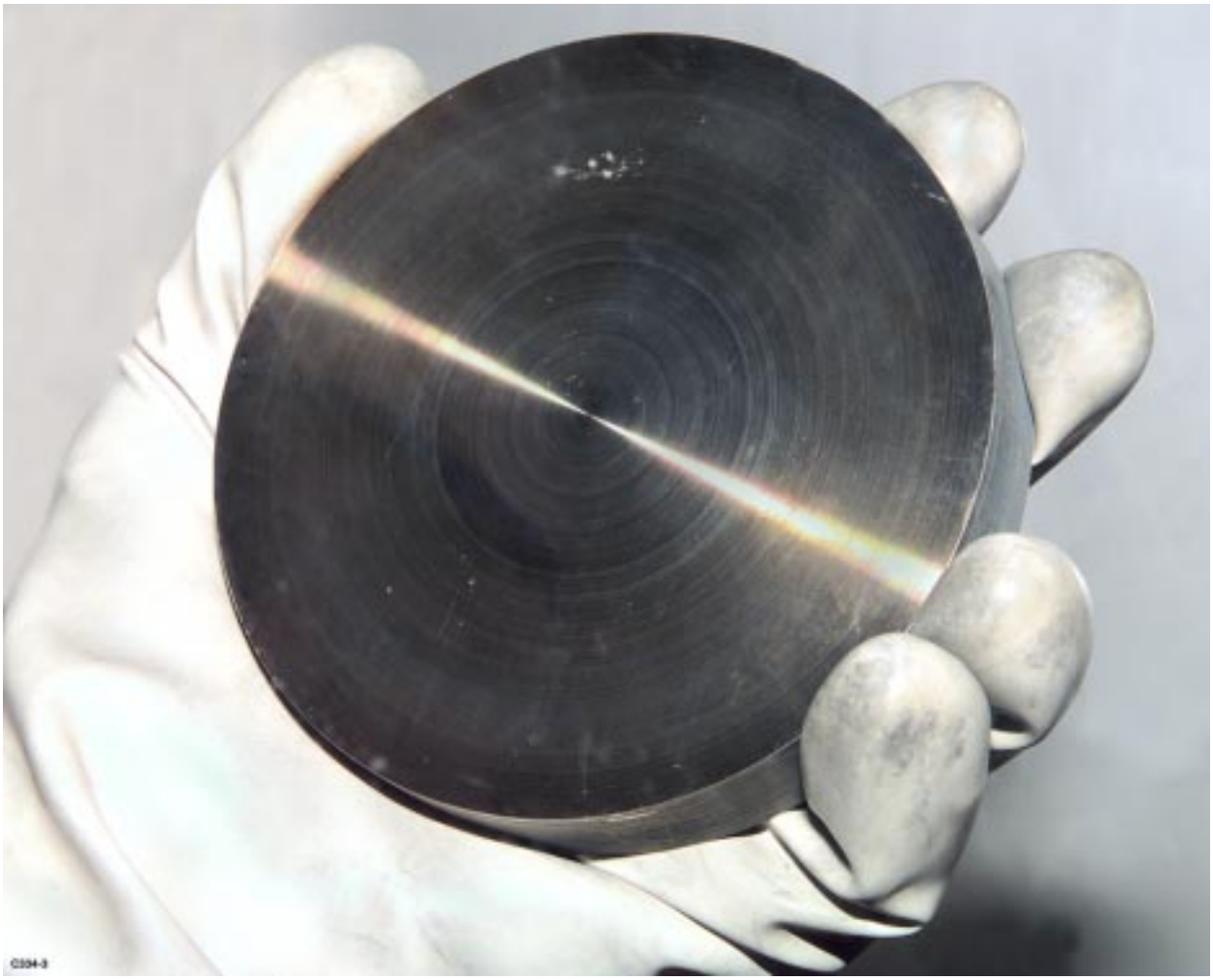

Figure 1 – Machined α-Pu ingot (4.358” diameter, 0.751” thick).

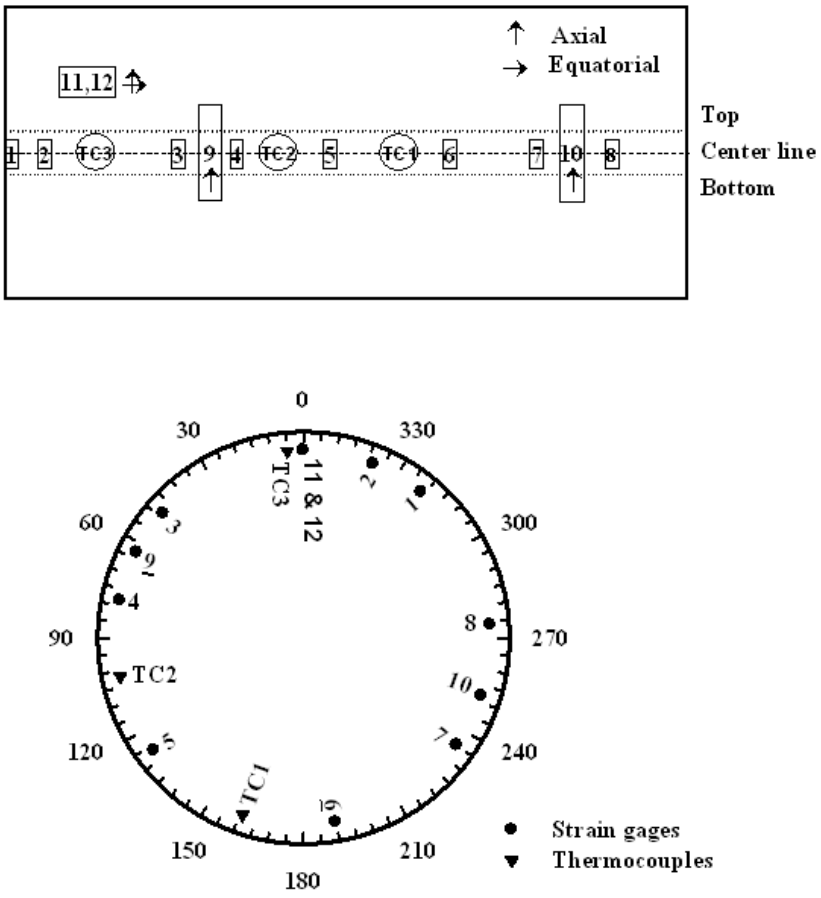

Figure 2 – Strain Gage and Thermocouple Locations
Top – cylinder unwrapped. *Bottom* – polar plot.
Gages 1-8 are oriented to measure strain in the equatorial direction.

Figure 3 – Close up of dilatometry set up. Note quartz rod attached to dial indicator.

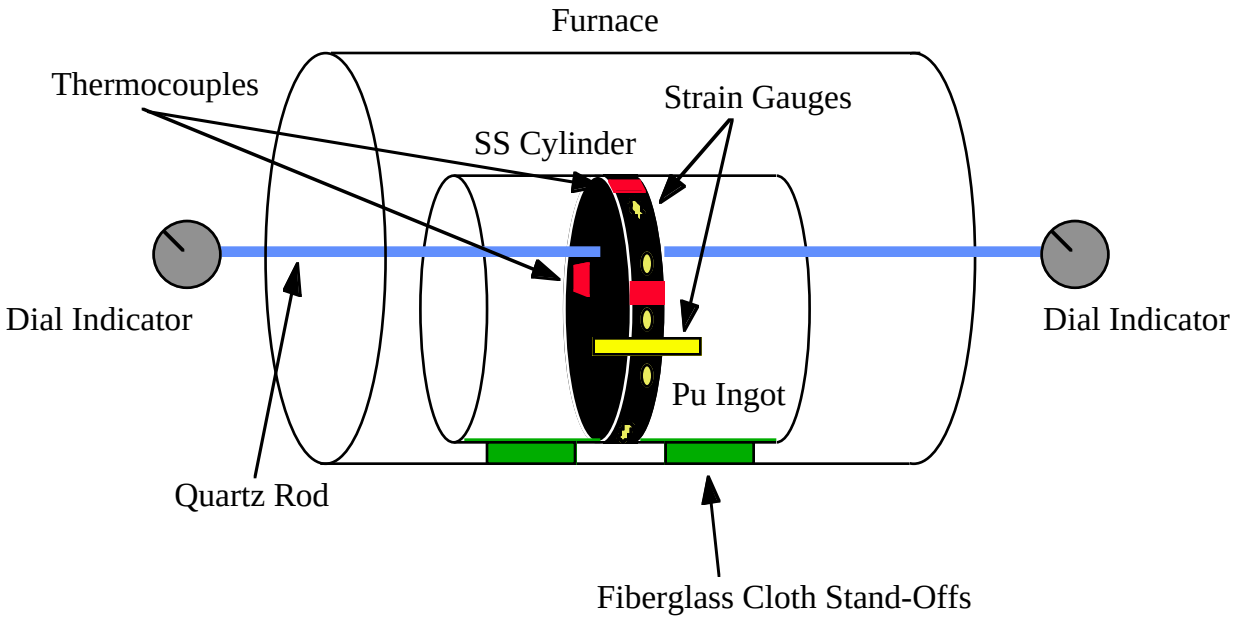

Figure 4 - Schematic of experimental set up. Not to scale.

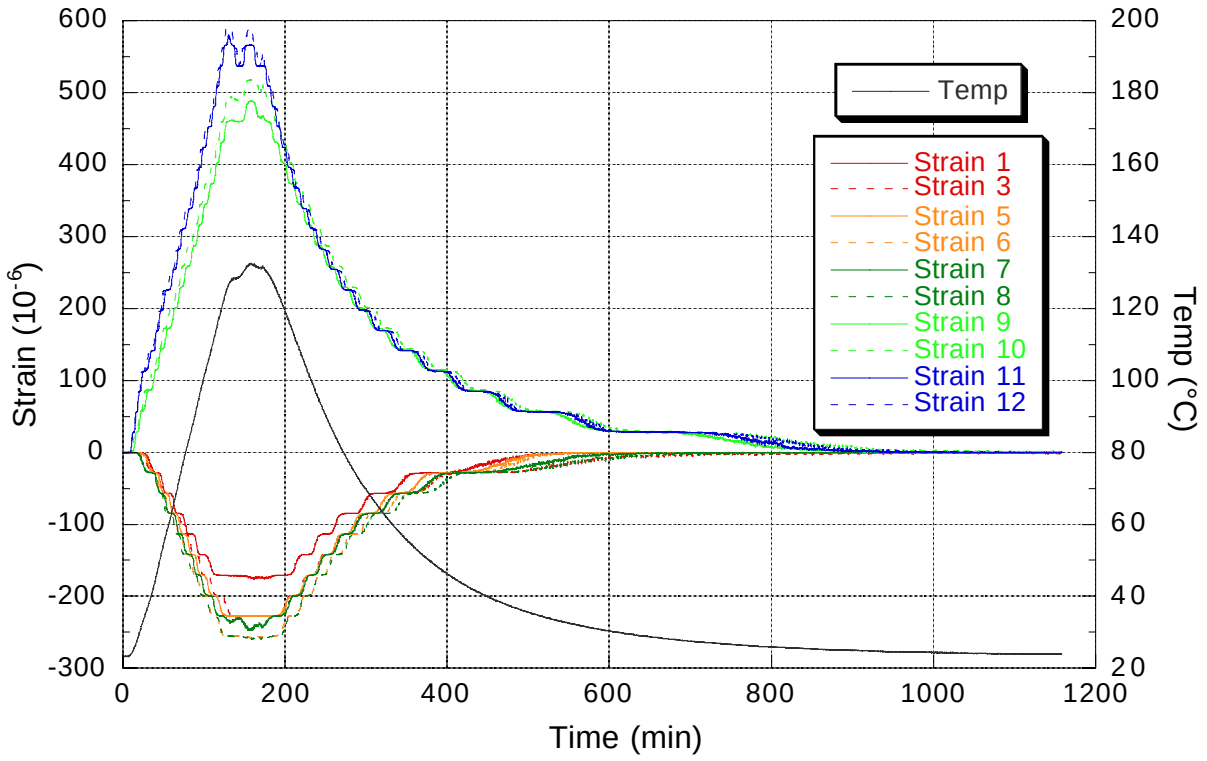

Figure 5 - Strain gage thermal with brass ingot. 30με steps are instrument resolution.

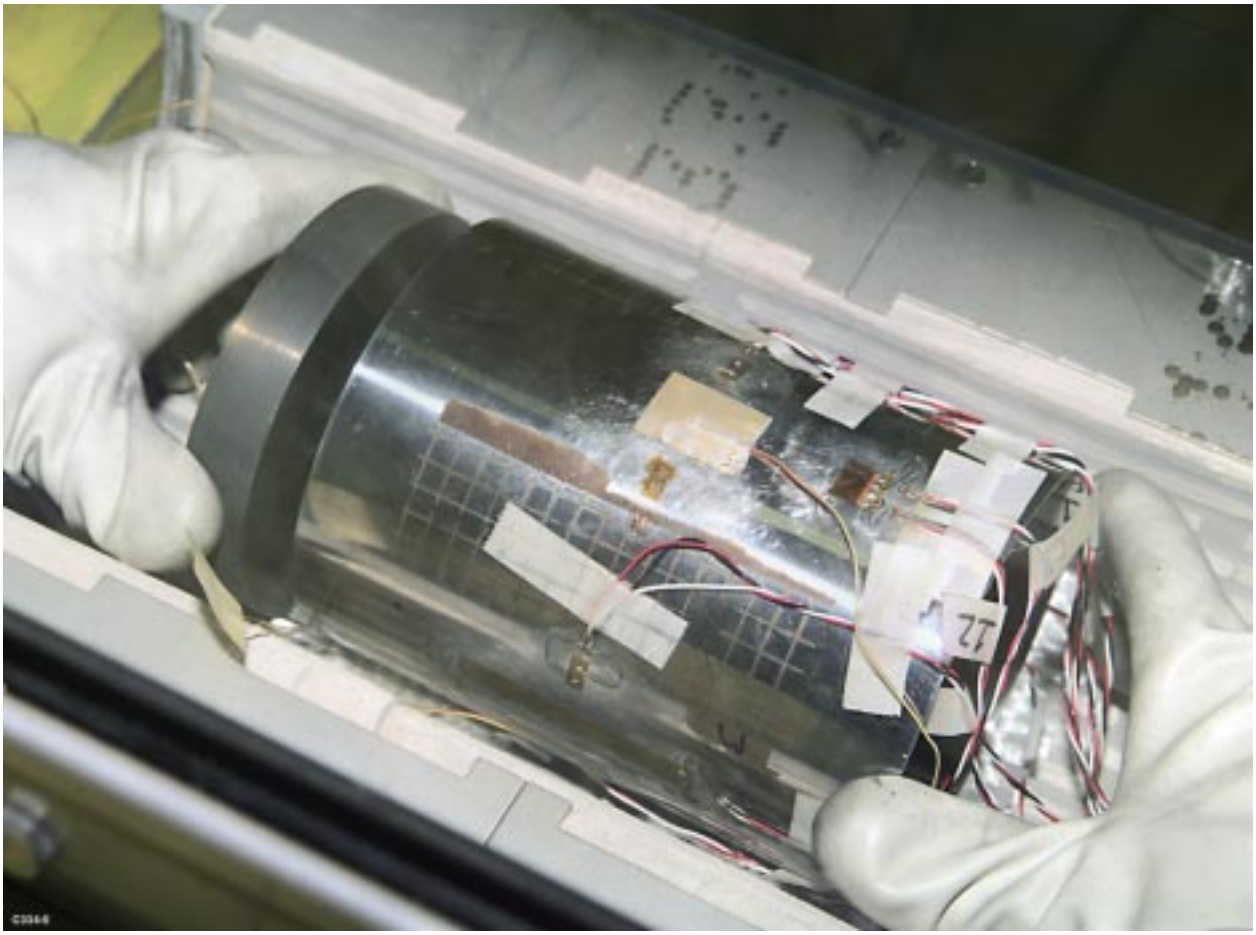

Figure 6 – Insertion of Pu ingot into stainless steel cylinder. Note strain gages and thermocouples on outside of cylinder.

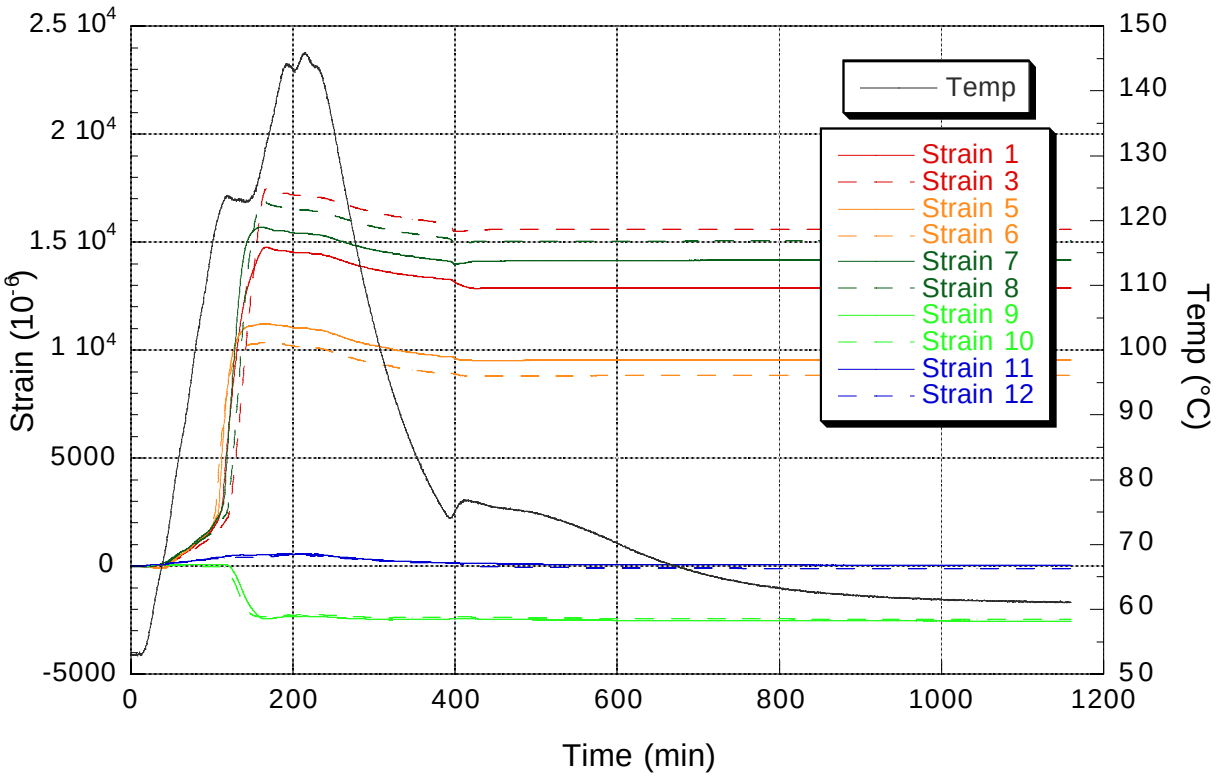

Figure 7
Cycle 1 Strain/Temp vs. Time

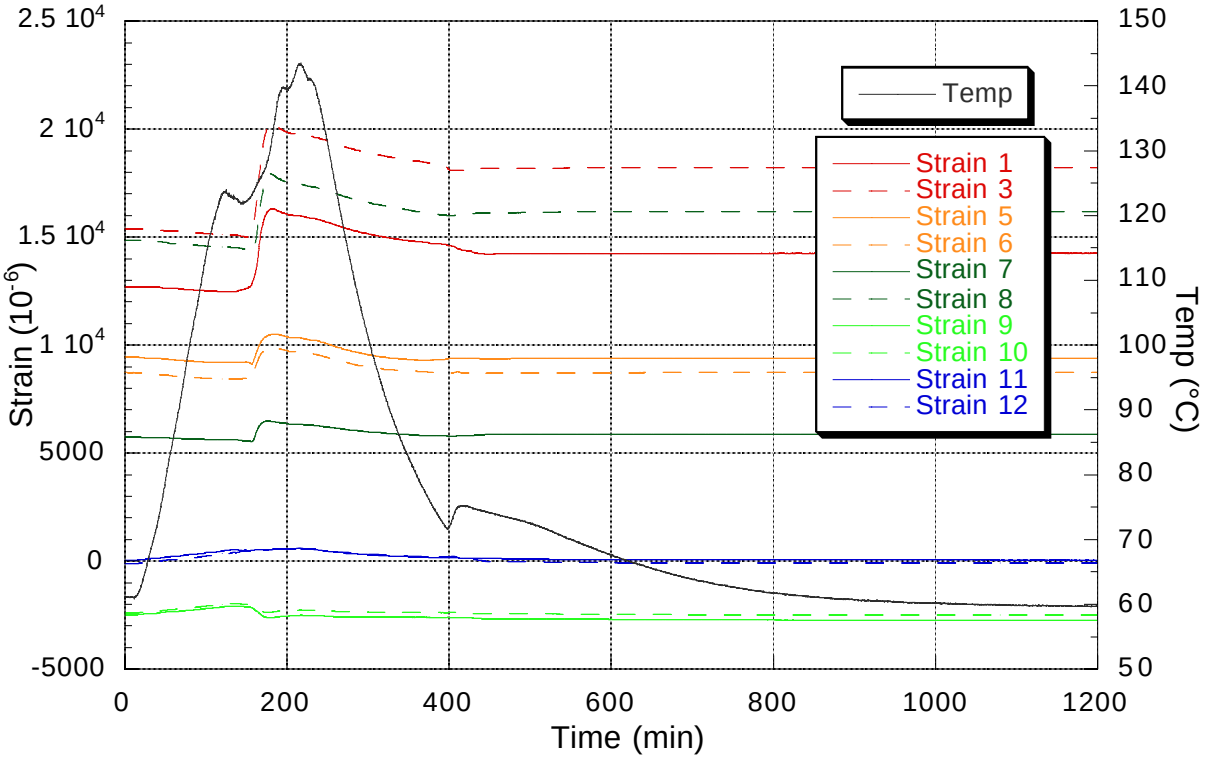

Figure 8
Cycle 2 – Strain/Temp vs. Time

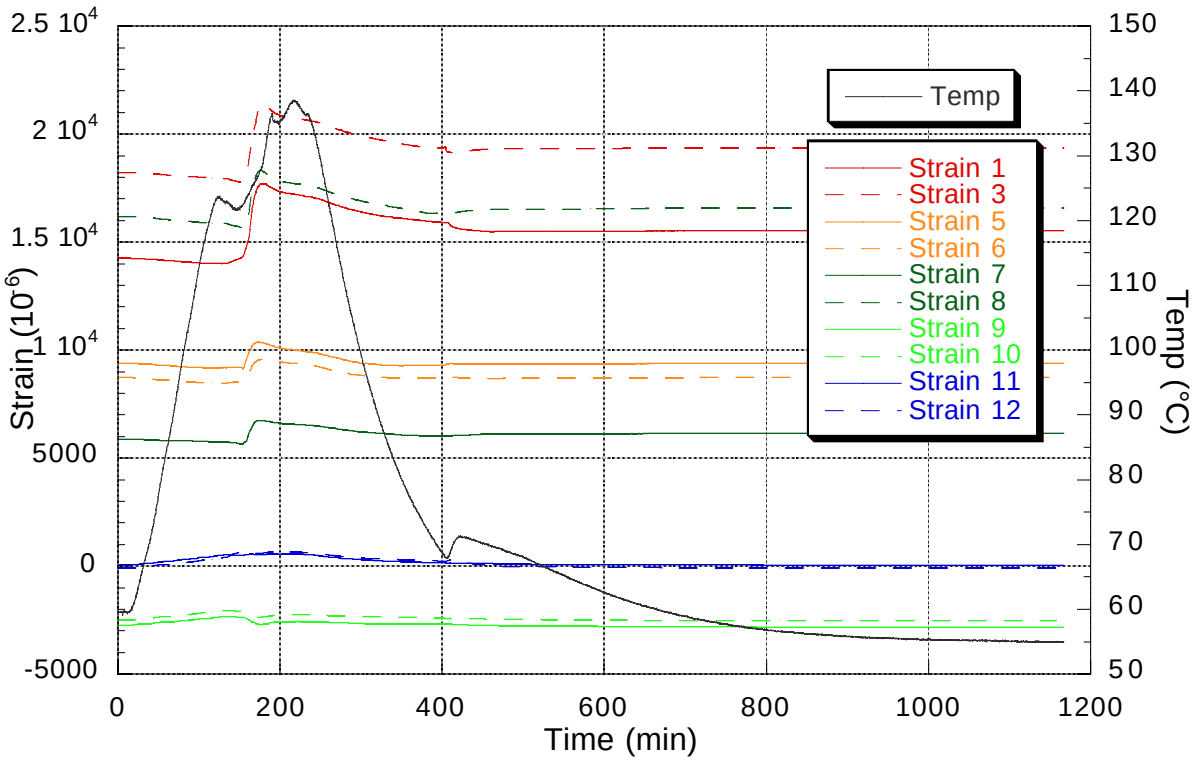

Figure 9
Cycle 3 – Strain/Temp vs. Time

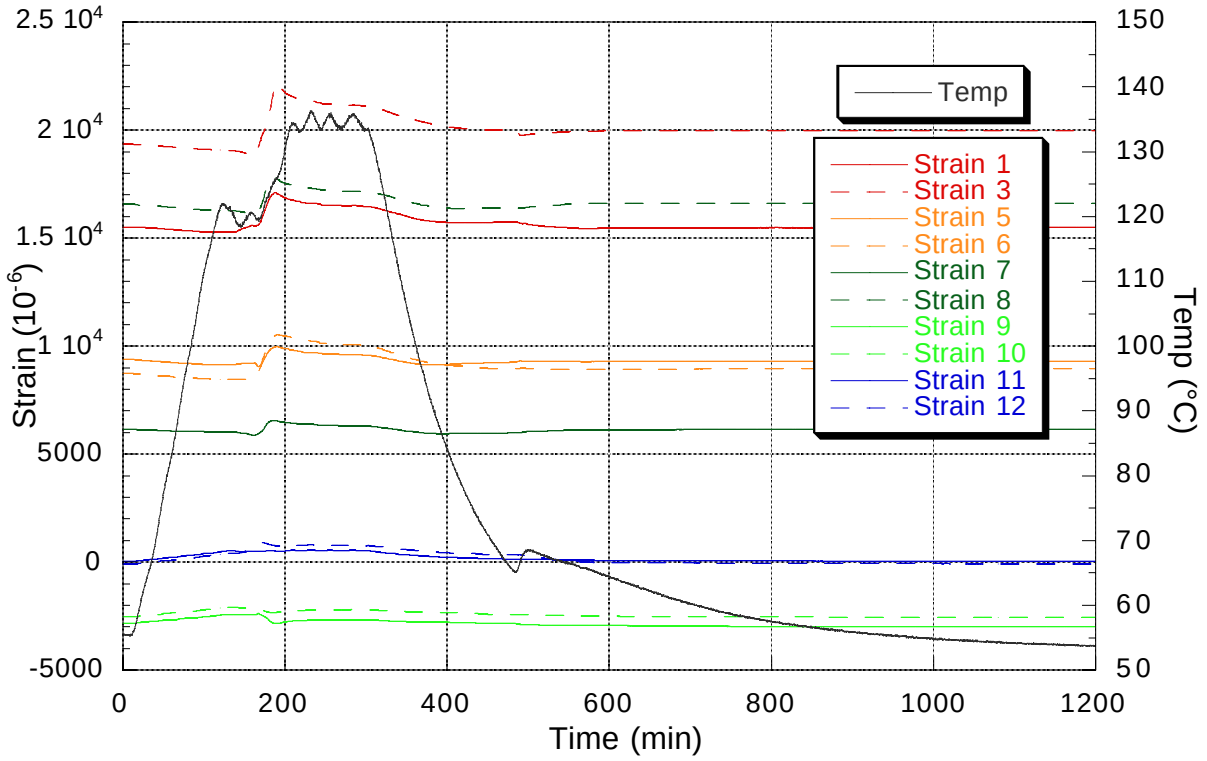

Figure 10
Cycle 4 – Strain/Temp vs. Temp

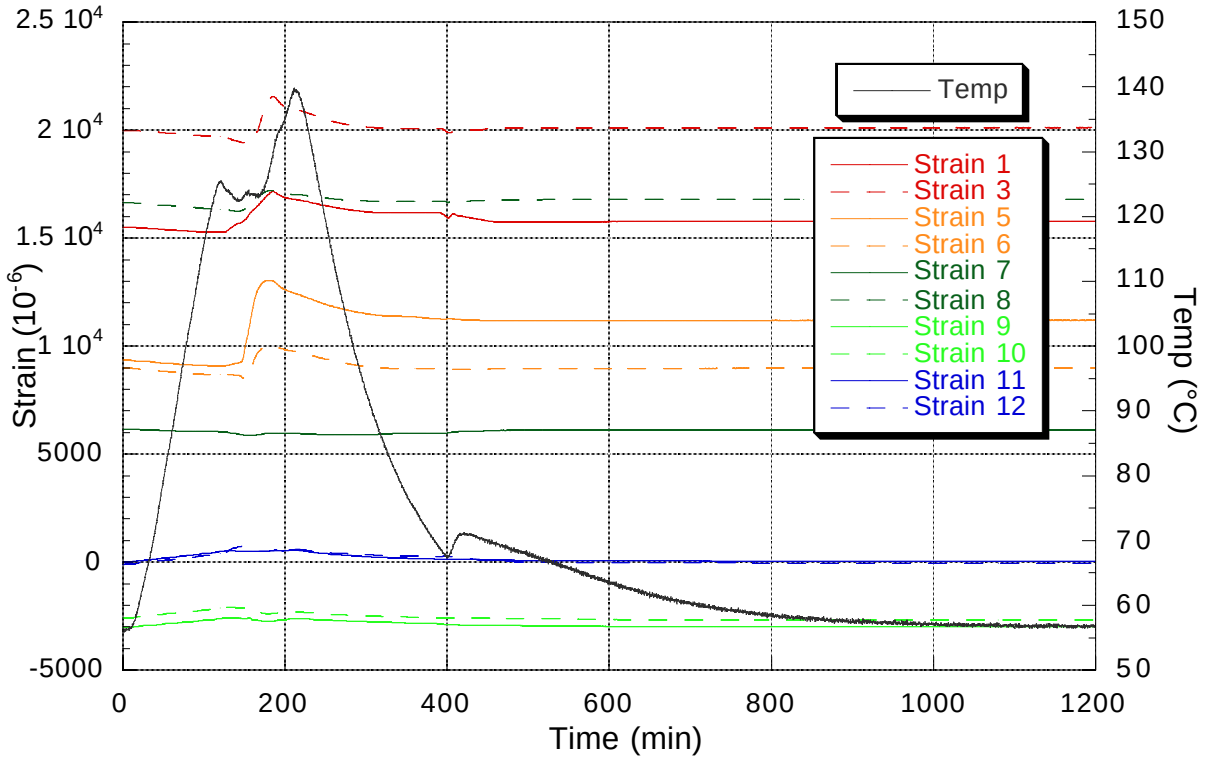

Figure 11
Cycle 5 – Strain/Temp vs. Time

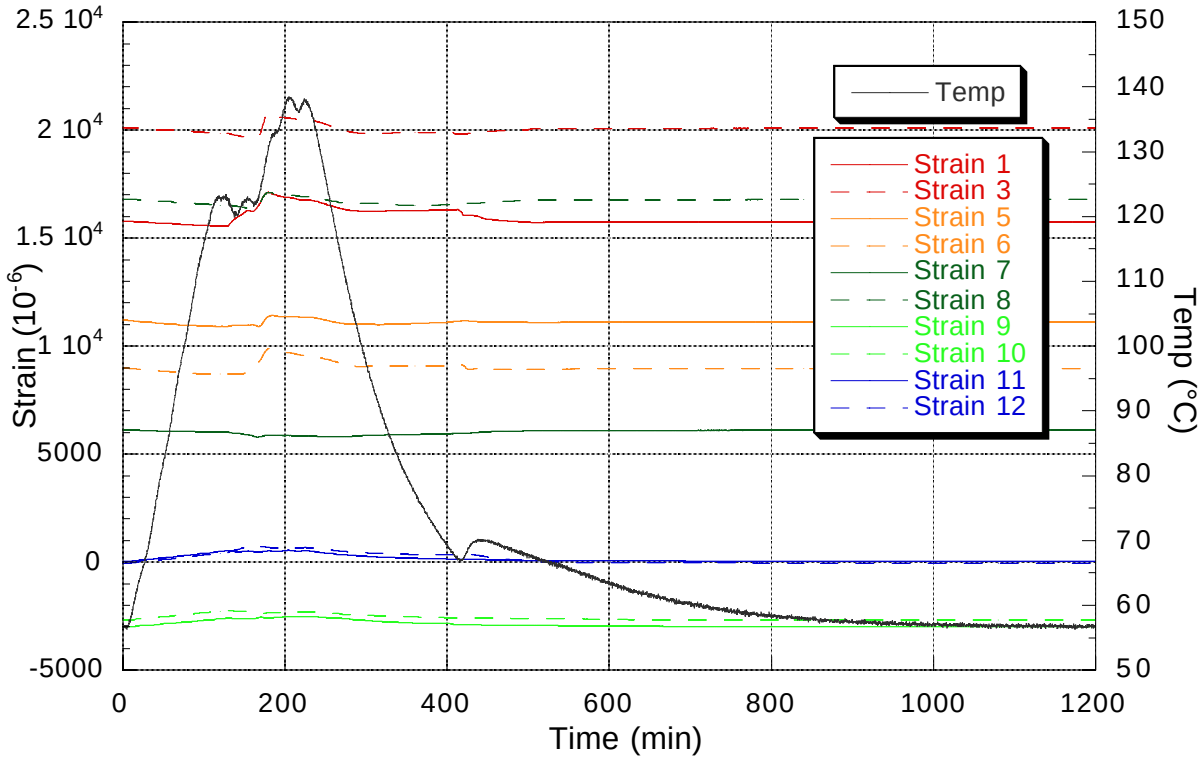

Figure 12
Cycle 6 – Strain/Temp vs. Time

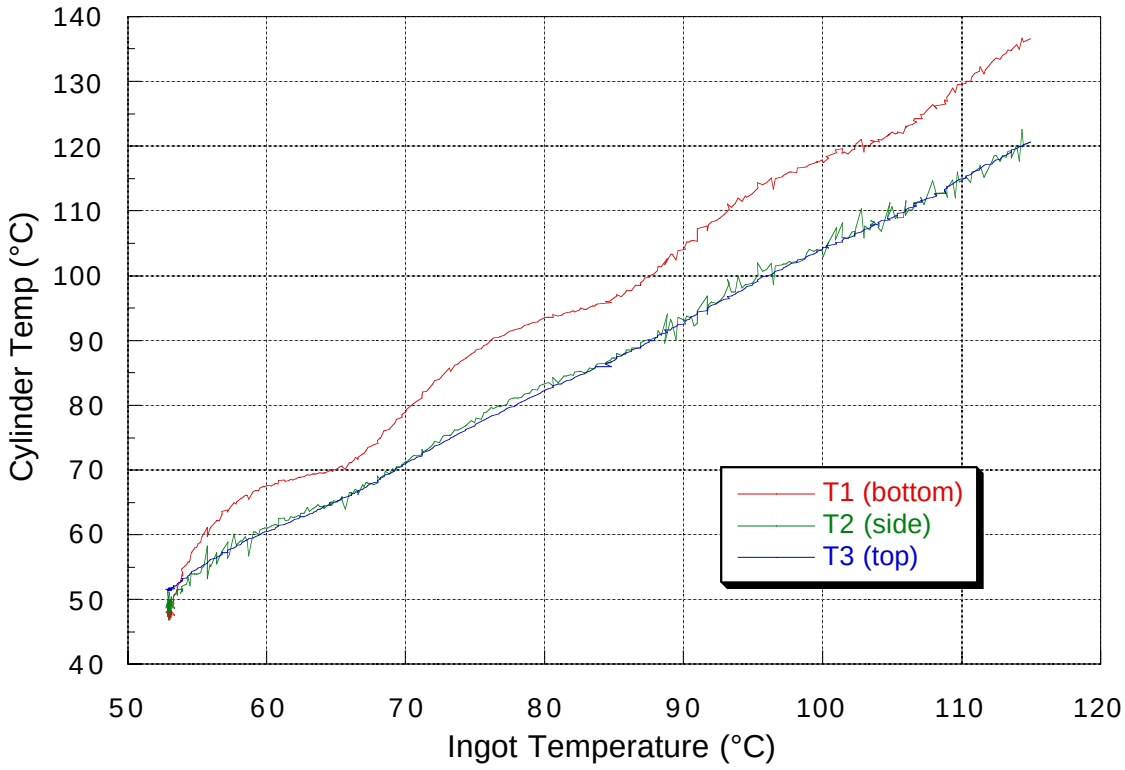

Figure 13 – Cylinder Temperatures vs. Ingot Temperature for Cycle 1

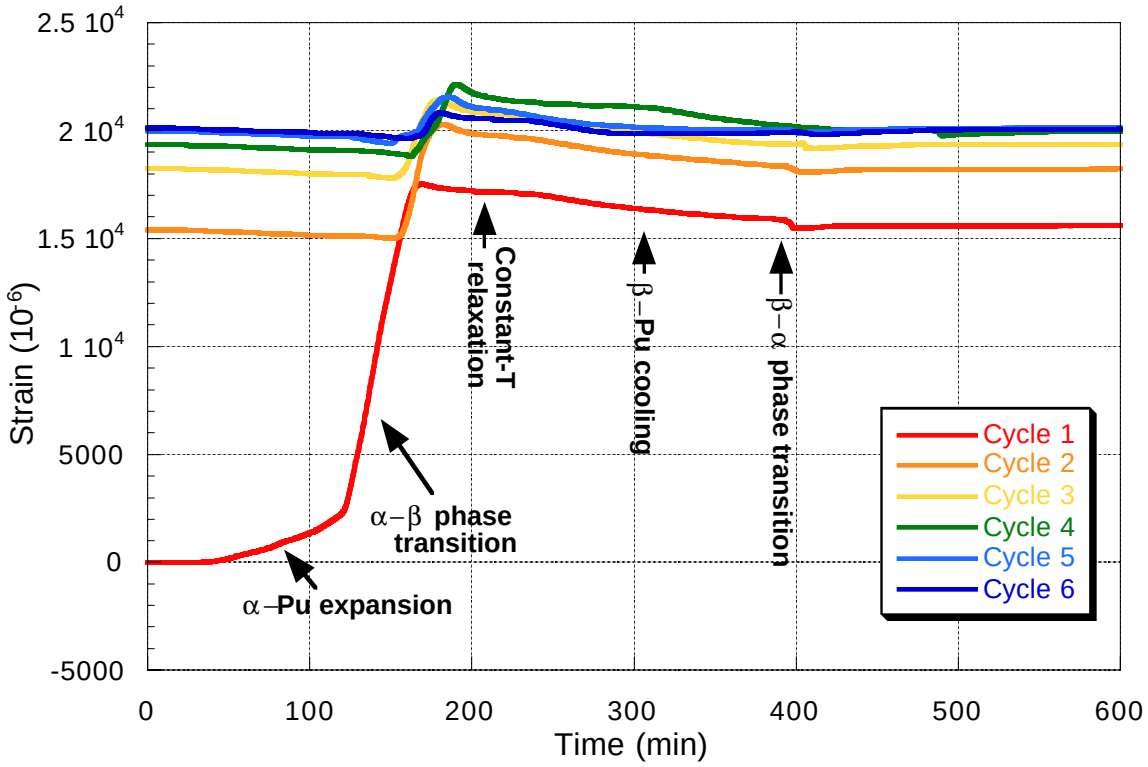

Figure 14 - Strain vs. Time response of strain gage #3 for all cycles.

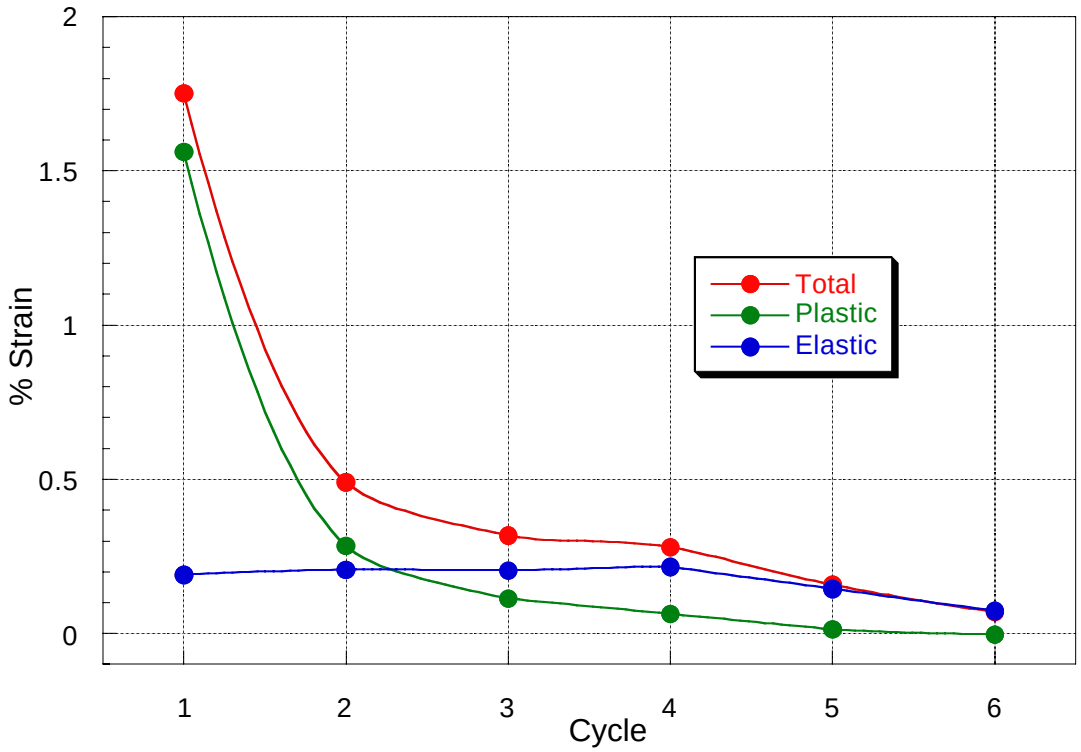

Figure 15 – Highest observed strain (from gage #3) vs. cycle.

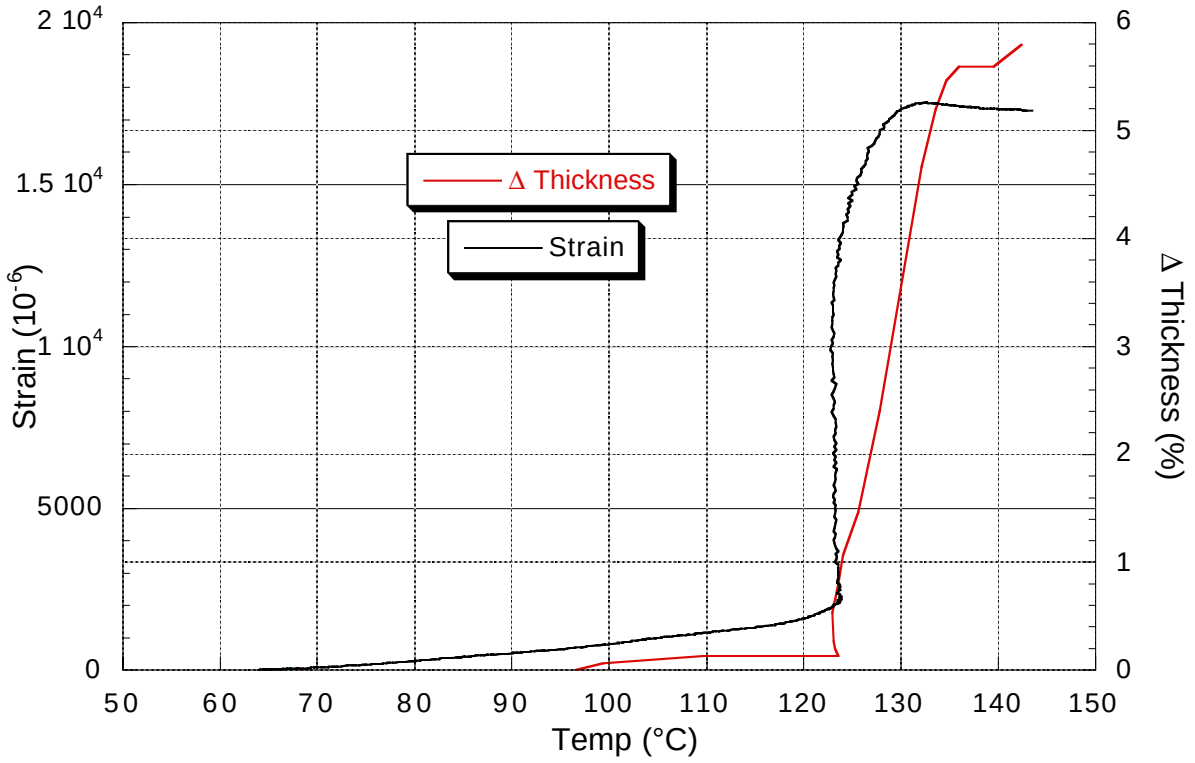

Figure 16 - Strain/Thickness vs Temp, first cycle, temp increasing.

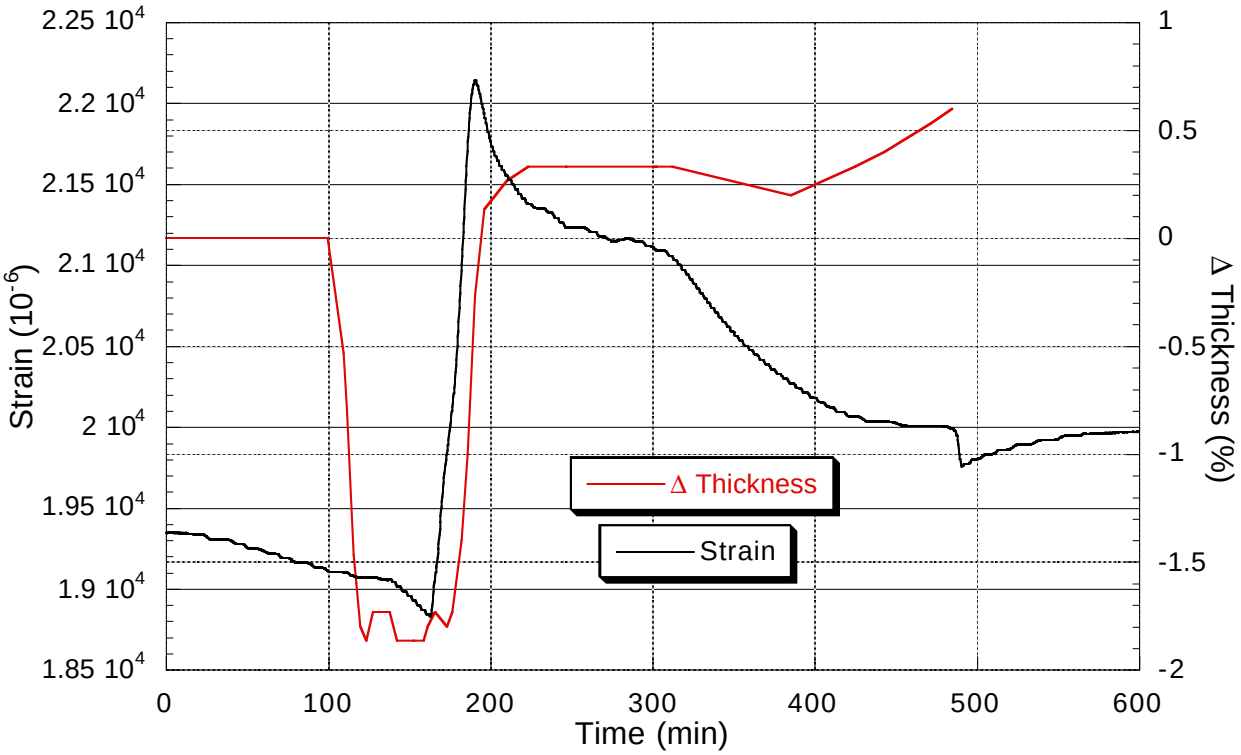

Figure 17 – Strain/Thickness vs Time, fourth cycle.

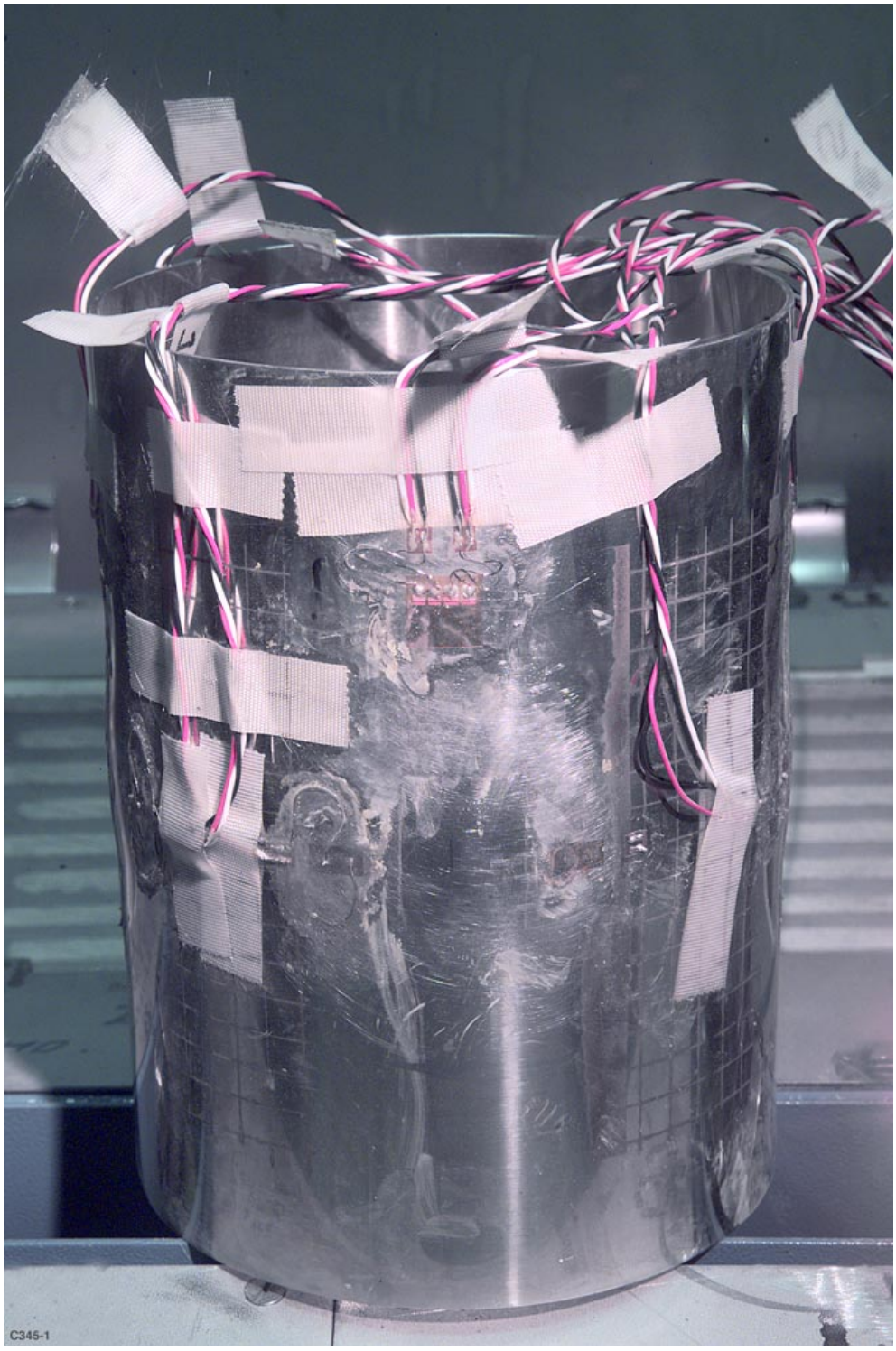

Figure 18 – Cylinder after six thermal cycles. Note plastic deformation around center of cylinder. Cylinder is 6” in length.

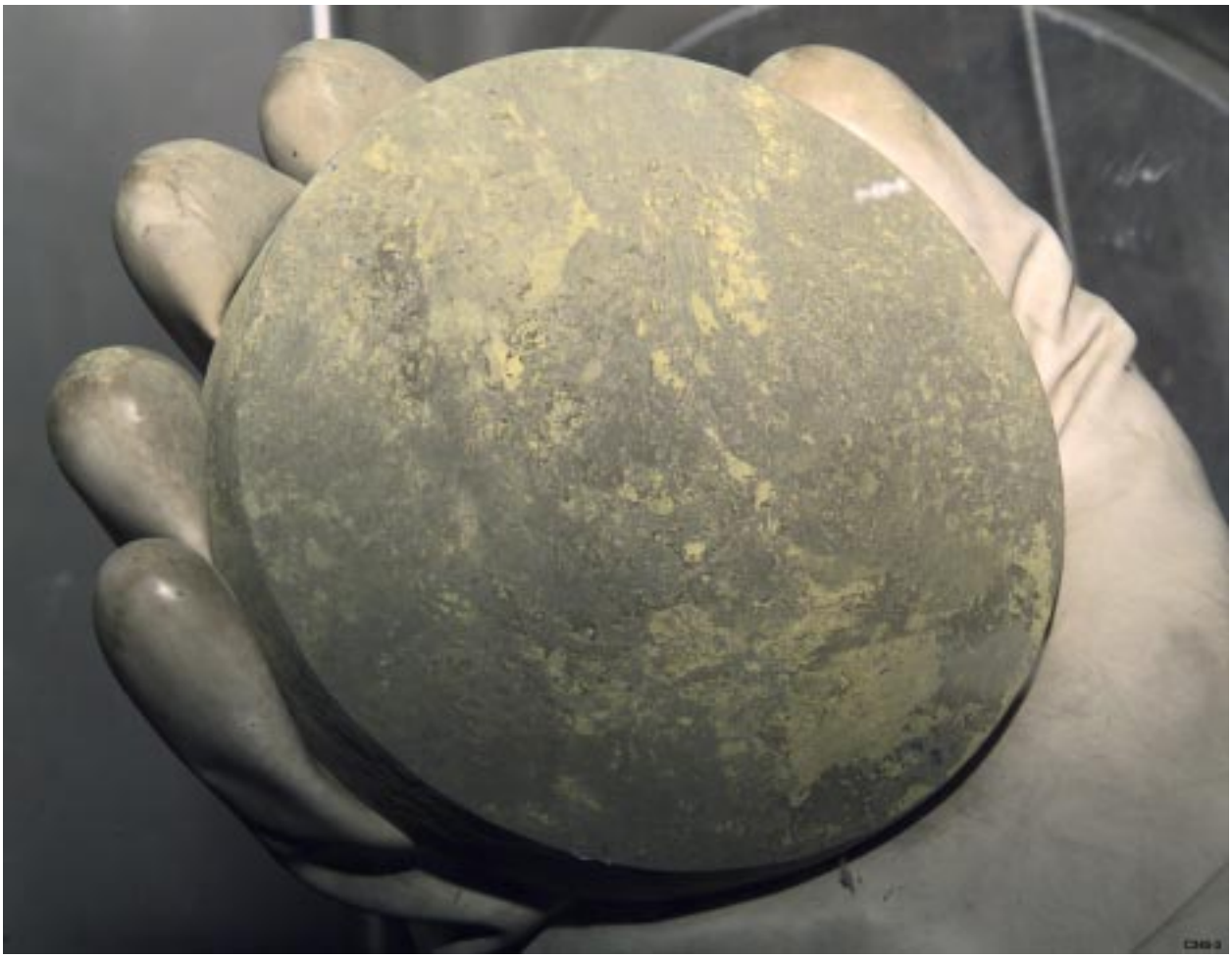

Figure 19 – Pu ingot after six thermal cycles showing moderate surface oxidation.